Macromolecules

ARTICLE

pubs.acs.org/Macromolecules

Self-Assembly into Multicompartment Micelles and Selective Solubilization by Hydrophilic−Lipophilic−Fluorophilic Block Copolymers

Jean-Noël Marsat,[†] Matthias Heydenreich,[†] Erich Kleinpeter,[†] Hans v. Berlepsch,[*,‡] Christoph Böttcher,[‡] and André Laschewsky[*,†,§]

[†]Department of Chemistry, Universität Potsdam, Karl-Liebknecht-Str. 24-25, D-14476 Potsdam-Golm, Germany

[‡]Forschungszentrum für Elektronenmikroskopie, Institut für Chemie und Biochemie, Freie Universität Berlin, Fabeckstr. 36a, D-14195 Berlin, Germany

[§]Fraunhofer Institute for Applied Polymer Research, D-14476 Potsdam-Golm, Germany

Supporting Information

ABSTRACT: Amphiphilic linear ternary block copolymers (ABC) were synthesized in three consecutive steps by the reversible addition−fragmentation chain transfer (RAFT) method. Using oligo(ethylene oxide) monomethyl ether acrylate, benzyl acrylate, and 1*H*,1*H*-perfluorobutyl acrylate monomers, the triblock copolymers consist of a hydrophilic (A), a lipophilic (B), and a fluorophilic (C) block. The block sequence of the triphilic copolymers was varied systematically to provide all possible variations: ABC, ACB, and BAC. All blocks have glass transition temperatures below 0 °C. Self-assembly into spherical micellar aggregates was observed in aqueous solution, where hydrophobic cores undergo local phase separation into various ultrastructures as shown by cryogenic transmission electron microscopy (cryo-TEM). Selective solubilization of substantial quantities of hydrocarbon and fluorocarbon low molar mass compounds by the lipophilic and fluorophilic block, respectively, is demonstrated.

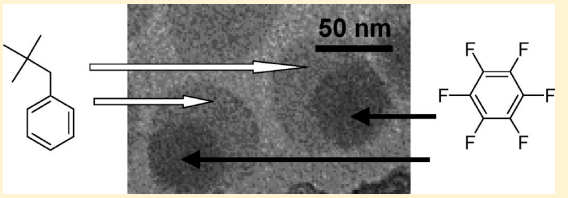

INTRODUCTION

Recent years have seen a continuous increase of interest in block copolymers and their self-assembly in bulk as well as in solution.[1−5] This interest is directly related to the improved synthetic methods such as living or controlled polymerizations, in particular the so-called "controlled free radical polymerization" methods that allow for the preparation of functional and hydrophilic blocks without the need of protective group chemistry.[6−9] Whereas the self-assembly of binary amphiphilic block copolymers in aqueous solution into a wealth of colloidal aggregates has been investigated intensely, studies on the self-assembly of amphiphilic ternary block copolymers are much less common.[10−22] Not only their synthesis faces several practical problems but also the molecular analysis is far from trivial. Nonetheless, ternary block copolymers with three incompatible blocks have been made and shown to self-organize into a variety of complex supramolecular structures, thus rendering them most interesting objects for fundamental studies.[14,23−25] The combination of one hydrophilic with two mutually incompatible hydrophobic blocks is particularly attractive, as such tercopolymers may form aggregates with internally compartmentalized hydrophobic microdomains.[26−28] Although only few examples of polymeric multicompartment micelles have been reported, a surprising variety of architectures for such systems have been explored employing amphiphilic comb block copolymers,[29−32] amphiphilic miktoarm structures,[33−37] hyperbranched star block copolymers,[38] and linear multiblock polymers.[15,18,20,28,39−47] The latter architectures offer the possibility to modify the self-assembly behavior not only by variation of the nature of the individual blocks and their relative sizes but also by changing the block sequence within the macromolecules.[28,44] Additionally, hydrophobically end-capped hydrophilic polymers with short fluorocarbon and hydrocarbon end groups have been studied in the context of multicompartment micelles.[39,48−51]

Beyond the exploration of new and unusual nanostructured systems, the interest in multicompartment systems has been stimulated by the option to accommodate different host compounds selectively and independently into distinct hydrophobic microdomains. In fact, the simplified functional analogy to transport proteins in the blood, such as serum albumin, had originally incited the topic of multicompartment systems.[26,27,52] Within this line of consideration, the mutual incompatibility and the resulting microphase separation into three distinct domains, one hydrophilic and two hydrophobic ones, is only a prerequisite, while the final focus is on the selective affinity of the different compartments for low molar mass compounds, namely water and two different hydrophobic species.[28,53] Hence, the term "triphilic" was coined for such type of compounds.[54,55] However,

Received: January 11, 2011
Revised: February 7, 2011
Published: March 02, 2011

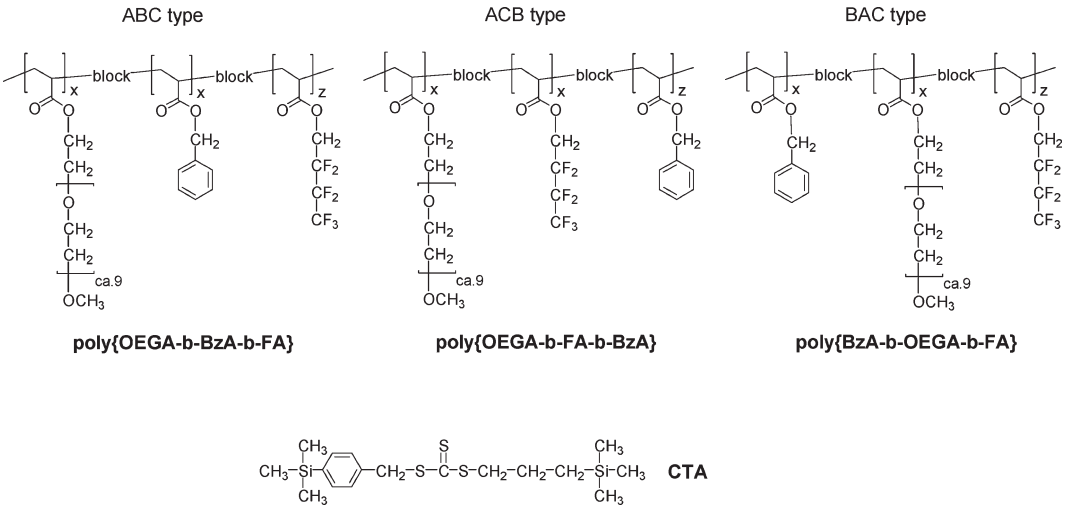

Figure 1. Chemical structures of the ternary block copolymers made and the RAFT agent used.

while a certain number of structural studies on the nanostructuring of amphiphilic ternary block copolymers with incompatible hydrophobic blocks has been reported in the meantime,[15,17,20,33−36,40−45,56−61] and quite some theoretical thought has been given to the topic,[24,52,62−69] studies on the triphilic behavior have been seldom performed so far, for instance studies on selective solubilization of sets of complementary hydrophobic substances.[28,29,31,70,71] The scarcity of such studies might be also reflected by two fundamental difficulties regarding true triphilic systems. First, the self-organization into three different microdomains does not necessarily imply that these domains can mutually distinguish between different low molar mass solutes. In fact, a high contrast in the interactions, as is reflected by strongly differing Hansen solubility parameters,[72] between the distinct hydrophobic domains is needed. Second, effective uptake of guest compounds asks for mobility and "voids" within the hydrophobic microdomains. It is well established that in the case of micellar solubilization the hydrophobic segments of the surfactants should be liquidlike to solubilize hydrophobic compounds efficiently.[73] In analogy, one may expect that semicrystalline or glassy polymer blocks are much less suited for effective and selective solubilization than blocks in the elastomeric or molten state. However, many studies on the formation of multicompartment colloids in aqueous systems have used at least one "hard" hydrophobic block, i.e., a block with high glass transition temperature or of semicrystalline character, which favors microphase separation.[15,42,44]

Within the described context, we are exploring the internal compartmentalization of polymeric micelles, using linear ternary block copolymers.[28] In order to achieve efficient microphase separation as well as selective solubilization of guest molecules, the incompatibility of the hydrophobic domains is achieved by the use of hydrocarbon and fluorocarbon building blocks. Accordingly, we are developing triphilic systems consisting of hydrophilic, lipophilic, and fluorophilic blocks, in the following referred to as A-, B-, and C-blocks, respectively. Following initial studies of such block copolymers made by the RAFT (radical addition−fragmentation chain transfer) method[6] on the basis of acrylate monomers,[41,42,44] we have now extended the previous polymer designs by replacing the semicrystalline fluorophilic C block with an amorphous one, while maintaining a "soft" lipophilic B block with low glass transition (Figure 1). Crystallization of the fluorophilic block was suppressed by substantial shortening of the long perfluoroalkyl side chains employed hitherto,[42,44] namely by replacing a perfluorooctyl with a perfluoropropyl residue. Accordingly, it was not clear whether this molecular design was still effective for multicompartmentalization and whether sufficient compatibility contrast could be achieved for cryo-TEM visualization. Therefore, increased polarity was conferred to the lipophilic block by replacing the formerly used alkyl chains by the benzyl residue. We expected that this design would suffice not only to induce microphase separation between the hydrophobic blocks but also to allow selective uptake of hydrocarbon and fluorocarbon compatible guest molecules. Preliminary results of such polymers were briefly mentioned in a recent feature article.[28] A direct consequence of the shorter fluoroalkyl residues in the fluorophilic block is an improved solubility in many solvents, which enabled the preparation and investigation of all possible block sequences ABC, BAC, and ACB. This had not been done before. Furthermore, we improved the notoriously difficult analysis of such copolymers by labeling the polymer end groups with two complementary NMR marker groups based on the trimethylsilyl (TMS) moiety.[74] The self-assembly of the new triphilic block copolymers of various block sequence in dilute aqueous solution was then explored by cryo-TEM, as well as by selective solubilization experiments.

EXPERIMENTAL PART

Methods. ^{1}H (300 MHz), ^{13}C (75 MHz), and ^{19}F NMR (282 MHz) spectra were taken with a Bruker Advance 300 apparatus. If not stated otherwise, all spectra are referenced to the respective solvent residual peak ($CHCl_3$ 7.26 ppm; D_2O 4.79 ppm). UV−vis spectra were recorded on a spectrophotometer Cary-1 (Varian), using quartz cuvettes (Suprasil, Hellma, Germany) with an optical path length of 10 mm. Thermal characterization by differential scanning calorimetry (DSC) used a DSC 822 differential scanning calorimeter (Mettler Toledo). Thermograms were run in a nitrogen atmosphere, applying heating−cooling−heating runs between −140 and 140 °C with rates of 5 K/min. The thermograms of the second heating ramp were analyzed. Dynamic light scattering (DLS) for the characterization of micellar solutions was performed with a high performance particle sizer (HPPS-ET, from Malvern Instruments, UK) equipped with a He−Ne laser (λ = 633 nm)

dx.doi.org/10.1021/ma200032j |*Macromolecules* 2011, 44, 2092–2105

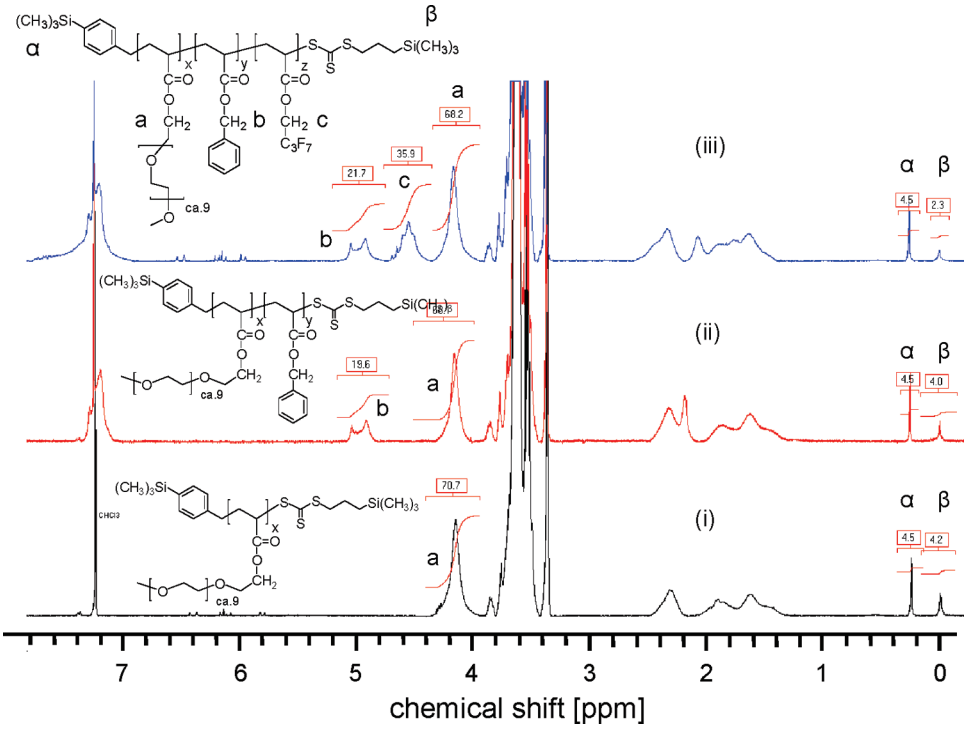

Figure 2. ^{1}H NMR spectra of (i) {$OEGA_{70}$}, (ii) {$OEGA_{70}$-BzA_{20}}, and (iii) {$OEGA_{70}$-BzA_{20}-FA_{35}} in $CDCl_3$.

and a thermoelectric Peltier element for controlling the temperature (temperature control range: 10−90 °C). The measurements were carried out at a scattering angle θ = 173° ("backscattering detection"). The autocorrelation functions were analyzed with the CONTIN method. The apparent hydrodynamic diameters D_h of micelles or aggregates were calculated according to the Stokes−Einstein equation, $D_h = kT/3\pi\eta D_{app}$, with D_{app} being the apparent diffusion coefficient and η the viscosity of the solution. Prior to measurements, the polymer solutions were filtered into a quartz glass cuvette (Suprasil, Hellma, Germany) with an optical path length of 10 mm using a WICOM OPTI-Flow 0.45 μm disposable filter. The samples for cryogenic transmission electron microscopy (cryo-TEM) were prepared at room temperature by placing a droplet (5 μL) of the solution on a hydrophilized perforated carbon filmed grid (60 s plasma treatment at 8 W using a BALTEC MED 020 device). The excess fluid was blotted off to create an ultrathin layer (typical thickness of 100 nm) of the solution spanning the holes of the carbon film. The grids were immediately vitrified in liquid ethane at its freezing point (−184 °C) using a standard plunging device. Ultrafast cooling is necessary for an artifact-free thermal fixation (vitrification) of the aqueous solution avoiding crystallization of the solvent or rearrangement of the assemblies. The vitrified samples were transferred under liquid nitrogen into a Philips CM12 transmission electron microscope using the Gatan cryoholder and cryostage (Model 626). Microscopy was carried out at −175 °C sample temperature using the microscopes low dose mode at a primary magnification of 58300× . The defocus was chosen to be 1.5 μm.

Micellar solutions were prepared by dissolving 10 mg of polymer in 2 mL of the common solvent acetone. Then 2 mL of distilled water was added dropwise under stirring. Subsequently, the acetone was evaporated for 24 h at ambient temperature. In annealing experiments, such solutions were stored at 75 °C for 2 weeks.

For solubilization experiments, 6 mg of polymer and 2 mL of D_2O are placed in a 4 mL vial and agitated for 24 h by a horizontal shaker (model IKA HS 501, 150 rpm) to give clear solutions. Then, 0.20 mL of neopentylbenzene or hexafluorobenzene were added, and the mixture was agitated for another 24 h. The excess of organic compound was allowed to phase separate and removed, before the transparent aqueous solutions were analyzed by NMR spectroscopy. The amount of solubilized neopentylbenzene (NPB) was calculated by comparing the integral of the signal of the *tert*-butyl moiety at 0.55 ppm in the ^{1}H NMR spectrum with the signal intensity at 4.2 ppm of the α-methylene ester group of the polyPEGA block (see Figure 2). The amount of solubilized hexafluorobenzene (HFB) was calculated by comparing the integral of the signal at 163.5 ppm in the ^{19}F NMR spectrum with the intensity of the signal at 75.9 ppm of a precise amount of sodium trifluoroacetate added to the solution as water-soluble internal standard. Experiments were carried out for all polymer solutions and the blank solvent references under the same experimental conditions. The values reported are averages over three experiments for each polymer, with a standard deviation of 20−30% of the mean values.

Materials. Oligo(ethylene glycol)methyl ether acrylate macromonomer (OEGA, M_r = 454, Aldrich) was purified by passing through a column filled with basic alumina (50−200 μm, Brockmann activity I, Acros) before use; benzyl acrylate (BzA, M_r = 162.19, 95%, ABCR) and 2,2,3,3,4,4,4-heptafluorobutyl acrylate (FA, M_r = 254.1, 97%, Acros) were vacuum-distilled and stored in a nitrogen atmosphere in the deep freezer. Tetrahydrofuran (THF, JTBaker) was distilled over K−Na alloy freshly before the use as solvent for the synthesis. Azobis(isobutyronitrile) (AIBN, 98%, Acros) was crystallized from ethanol. CH_2Cl_2 (99%, Merck), CCl_4 (99%, Acros), α,α,α-trifluorotoluene (TFT, 99%, Acros), (2,2-dimethylpropyl)benzene (NPB "neopentylbenzene", 98%, Acros), and hexafluorobenzene (HFB, 99%, Acros) were used as received. The synthesis of RAFT chain transfer agent 4-(trimethylsilyl)benzyl 4′-(trimethylsilyl)butane dithioate ($C_{17}H_{30}S_2Si_2$, M_r = 354.72), CTA, was described before.[74] Water used for the preparation of micellar solutions was purified by a Millipore Q Plus water purification system (resistivity of 18 MΩ·cm). Dialysis used cellulose membranes (Zellutrans, Roth, nominal cutoff 3500 MCWO 4000−6000).

Synthesis of the Homopolymers PolyOEGA. In a typical procedure, 0.160 g (4.40 × 10^{-4} mol) of CTA and OEGA (18.4 mL, 20 g, 4.6 × 10^{-2} mol) were dissolved in 90 mL of distilled THF and purged with nitrogen for 30 min. The flask was immersed in an oil bath and heated to

Table 1. Polymerization Conditions, Using AIBN as Initiator (Reaction Temperature 70 °C)

entry no.	polymer	RAFT agent used	monomer	AIBN [mg]	solvent	reaction time [h]	yield [%]
1	{$PEGA_{70}$}	CTA, 0.16 g	OEGA, 20.0 g	7	THF, 100 mL	4	68
2	{$PBzA_{45}$}	CTA, 0.43 g	BzA, 20.0 g	19	THF, 50 mL	5	52
3	{PFA_{15}}	CTA, 0.05 g	FA, 1.20 g	2	TFT, 10 mL	5	49
4	{$OEGA_{70}$-BzA_{20}}	entry 1, 2.00 g	BzA, 0.45 g	2	THF,10 mL	5	41
5	{$OEGA_{70}$-FA_{10}}	entry 1, 2.00 g	FA, 0.63 g	2	TFT, 10 mL	5	20
6	{BzA_{45}-$OEGA_{175}$}	entry 2, 0.40 g	OEGA, 2.50 g	2	THF, 10 mL	5	73
7	{BzA_{45}-FA_{60}}	entry 2, 1.00 g	FA, 1.74 g	2	TFT, 5 mL	10	80
8	{$OEGA_{70}$-BzA_{20}-FA_{35}}	entry 4, 0.50 g	FA, 0.14 g	2	TFT, 5 mL	10	70
9	{$OEGA_{70}$-FA_{10}-BzA_{25}}	entry 5, 0.50 g	BzA, 0.10 g	2	TFT, 5 mL	5	60
10	{BzA_{45}-$OEGA_{175}$-FA_{40}}	entry 6, 0.50 g	FA, 0.07 g	2	TFT, 5 mL	10	78
11	{$OEGA_{40}$}	CTA, 0.16 g	OEGA, 20.0 g	7	benzene, 100 mL	4	41
12	{$OEGA_{40}$-BzA_{45}}	entry 11, 2.00 g	BzA, 2.26 g	2	benzene, 20 mL	5	45
13	{$OEGA_{40}$-FA_{30}}	entry 11, 2.00 g	FA, 1.78 g	2	TFT, 10 mL	10	60
14	{BzA_{45}-$OEGA_{40}$}	entry 2, 2.00 g	OEGA, 6.20 g	2	benzene, 40 mL	5	79
15	{$OEGA_{40}$-BzA_{45}-FA_{30}}	entry 12, 0.50 g	FA, 0.30 g	2	TFT, 5 mL	10	62
16	{$OEGA_{40}$-FA_{30}-BzA_{45}}	entry 13, 0.50 g	BzA, 0.25 g	2	TFT, 5 mL	5	46
17	{BzA_{45}-$OEGA_{40}$-FA_{30}}	entry 14, 0.50 g	FA, 0.30 g	2	TFT, 5 mL	10	61

70 °C. AIBN (7.0 mg, 4.4×10^{-5} mol) in 10 mL of distilled THF was injected into the reaction mixture via a syringe through a septum. After 4 h, the polymerization was quenched by placing the flask into an ethanol/dry ice bath at −78 °C. The THF was removed by rotary evaporation. A sample was taken at that point to determine the conversion by ^{1}H NMR spectroscopy (conversion after 4 h: 68%). The residual monomer was removed from the polymer by dialysis in water for 6 days. The dialyzed solution was freeze-dried to give the final product as yellow viscous mass, yield 68%.

Synthesis of the Homopolymers PolyBzA. In a typical procedure, benzyl acrylate, BzA (9.3 mL, 10.00 g; 0.120 mol), and CTA (0.430 g, 1.2×10^{-3} mol) were dissolved in 40 mL of distilled THF and purged with nitrogen for 30 min. The flask was immersed in an oil bath and heated to 70 °C. AIBN (19 mg, 1.2×10^{-4} mol) in 10 mL of distilled THF was injected into the reaction mixture via a syringe through a septum. After 5 h, the polymerization was quenched by placing the flask into an ethanol/dry ice bath at −78 °C. After evaporating the THF, conversion was determined by ^{1}H NMR spectroscopy (52% conversion after 5 h), and the polymer poly{BzA} was precipitated thrice into cold hexane and dried in vacuum to give a yellow viscous mass, yield 52%.

Synthesis of the Diblock Copolymers. In a typical procedure for poly{OEGA-*b*-BzA}, macro-chain-transfer agent {$OEGA_{70}$} (2.00 g, 6.3×10^{-5} mol) dissolved in THF (9 mL) was placed in a 50 mL Schlenk tube equipped with a stirrer. After adding BzA (0.450 g, 2.8×10^{-3} mol), the mixture was stirred and purged for 20 min with nitrogen to give a homogeneous mixture. The flask was immersed in an oil bath and heated to 70 °C. AIBN (2.0 mg, 1.2×10^{-5} mol) in 1 mL of THF was injected into the reaction mixture via a syringe. After 5 h, the polymerization was quenched by placing the flask into an ethanol/dry ice bath at −78 °C. After evaporating the THF, conversion was determined by ^{1}H NMR spectroscopy (41% conversion after 5 h). Residual BzA was removed by dialysis in water/ethanol (mixture 40/60 v/v) for 3 days. After evaporating off the ethanol, the remaining aqueous solution was freeze-dried to give a yellow viscous mass, yield 41%.

Block copolymers poly{OEGA-*b*-FA}, poly{BzA-*b*-OEGA}, and poly{BzA-*b*-FA} were prepared following analogous procedures, using previously synthesized macroinitiators poly{OEGA} and poly{BzA}. THF or benzene was employed as solvent for polymerizing OEGA and BzA, while TFT was used for polymerizing FA. All polymers were purified by dialysis in ethanol/water (40/60 v/v).

Synthesis of the Triblock Copolymers. In a typical procedure for poly{OEGA-*b*-BzA-*b*-FA}, FA (0.140 g, 5.5×10^{-4} mol) and macro-chain-transfer agent poly{$OEGA_{70}$-BzA_{20}} (0.50 g, 1.4×10^{-5} mol) in TFT (9 mL) were placed in a 50 mL Schlenk tube equipped with a stirrer. The mixture was stirred and purged for 20 min with nitrogen to give a homogeneous solution. The flask was immersed in an oil bath and heated to 70 °C. Initiator solution (1 mL of a solution of AIBN (2.00 mg, 1.2×10^{-5} mol) in 10 mL of TFT, purged with nitrogen) was injected into the reaction mixture via a syringe through a septum. After 10 h, the polymerization was quenched by placing the flask into an ethanol/dry ice bath at −78 °C. The TFT was removed by rotary evaporation (70% conversion after 10 h according to NMR analysis), and the polymer was purified by dialysis in ethanol/water (40/60 v/v).

Poly{OEGA-*b*-FA-*b*-BzA} and poly{BzA-*b*-OEGA-*b*-FA} were synthesized analogously in TFT, employing the corresponding macro-RAFT agents poly{OEGA-*b*-FA} and poly{BzA-*b*-OEGA}. All polymers were purified by dialysis in ethanol/water (40/60 v/v).

Theoretically expected number-average molar masses M_n^{theo} of the polymers were calculated by eq 1, assuming ideal RAFT polymerization conditions,[75,76] i.e., neglecting AIBN initiated chains as well as any termination reaction.

$$M_n^{theo} = \alpha \times ([M]_0/[RAFT]_0) \times M + M_{RAFT} \quad (1)$$

where $[RAFT]_0$ is the engaged molar amount of RAFT agent, $[M]_0$ is the initial molar amount of monomer, M is the monomer's molecular mass, M_{RAFT} is the RAFT agent's molar mass, and α is the conversion. The latter was determined from ^{1}H NMR spectra of samples from the reaction mixture after evaporating the volatile solvents at ambient temperature and slightly reduced pressure.

Number-average molar masses M_n of the polymers were determined by end-group analysis via ^{1}H NMR spectroscopy, using the signal of the trimethylsilyl (TMS) group on the initiating benzyl fragment of CTA, the so-called R-group, introduced into the polymers (δ about 0.25 ppm). The intensity of this signal is compared to the intensity of the resolved signals of the $-CH_2-OOC-$ groups of the monomer units incorporated, at about 4.15 ppm (OEGA), 5.0 ppm (BzA), and 4.5 ppm (FA). The ratio of the intensities of the R-group signal at about 0.25 ppm and of the TMS moiety on the dithioester fragment (the so-called Z-group) at about 0 ppm was used to calculate the extent of end-group functionalization of the polymer chains with RAFT active Z-groups.

Table 2. Molecular Characteristics of the Ternary Triblock Copolymers Synthesized and of the Precursor Homopolymers and Diblock Copolymers

entry no.	polymer	macro-RAFT agent	$M_n^{theo\,a}$	M_n (NMR)^b	content of active Z-groups^c in %	M_n (UV)^d	M_n* (UV)^e
1	{$PEGA_{70}$}		34 000	32 000	93	39 000	36 000
2	{$PBzA_{45}$}		8 400	7 300	96	8 500	8 200
3	{PFA_{15}}		3 700	3 800	91	4 400	4 000
4	{$OEGA_{70}$-BzA_{20}}	1	37 000	35 000	88	41 000	36 000
5	{$OEGA_{70}$-FA_{10}}	1	36 000	34 000	67	58 000	39 000
6	{BzA_{45}-$OEGA_{175}$}	2	75 000	86 000	87	93 000	81 000
7	{BzA_{45}-FA_{60}}	2	23 000	22 000	69	36 000	25 000
8	{$OEGA_{70}$-BzA_{20}-FA_{35}}	4	46 000	44 000	51	87 000	45 000
9	{$OEGA_{70}$-FA_{10}-BzA_{25}}	5	41 000	38 000	53	82 000	43 000
10	{BzA_{45}-$OEGA_{175}$-FA_{40}}	6	85 000	97 000	87	104 000	91 000
11	{$OEGA_{40}$}		18 000	19 000	92	19 000	17 000
12	{$OEGA_{40}$-BzA_{45}}	11	25 000	27 000	91	26 000	24 000
13	{$OEGA_{40}$-FA_{30}}	11	27 000	26 000	85	33 000	28 000
14	{BzA_{45}-$OEGA_{40}$}	2	26 000	25 000	91	27 000	25 000
15	{$OEGA_{40}$-BzA_{45}-FA_{30}}	12	35 000	33 000	84	40 000	34 000
16	{$OEGA_{40}$-FA_{30}-BzA_{45}}	13	34 000	33 000	80	44 000	35 000
17	{BzA_{45}-$OEGA_{40}$-FA_{30}}	14	35 000	33 000	82	39 000	32 000

[a] Calculated via eq 1, conversion determined by ^{1}H NMR. [b] By ^{1}H NMR, using the relative signal intensities of the TMS R end group and the protons of the α-ester groups of the constitutional repeat units. [c] By ^{1}H NMR, according to the relative signal intensity of the TMS R and Z end groups. [d] From the absorbance of the dithioester UV band at 308 nm of the Z end group. [e] M_n(UV) values corrected by the content of active Z end group.

Alternatively, number-average molar masses M_n of the polymers were estimated from the UV-band of the intense $\pi-\pi$ transition of the thioester group at 308 nm in CH_2Cl_2 (extinction coefficient: ε = 10 864 L/(mol cm)), assuming the presence of exactly one Z-group in the polymers. In order to take the inevitable increasing loss of Z-groups with ongoing polymerization into account (resulting in an overestimation of the true M_n value), a value M_n*(UV) was additionally defined, which normalizes the values of M_n(UV) by the extent of end-group functionalization as obtained by ^{1}H NMR (see above).

RESULTS AND DISCUSSION

Terblock Copolymer Synthesis. The various polymers were prepared by sequential RAFT solution polymerizations. Note that all permutations of the triphilic block copolymers could be realized, i.e., the sequences ABC, BAC, and ACB (Figure 1). While THF or benzene was useful for polymerizing systems that contain only blocks made of OEGA and BzA, the fluorinated poly{FA} block is hardly soluble in these solvents, thus impeding homogeneous reactions. Therefore, TFT was used for all polymerizations, in which the fluorinated monomer or polymers were involved. The molar ratio of initiator AIBN/RAFT agent was 1:10 for the homopolymerizations and 1:10 or 1:5 for the synthesis of block copolymers. Reaction temperature and times were chosen such that initiator decomposition was limited to about 50% in the former case and to about 25% in the latter case at the end of the polymerizations. Accordingly, the number of inherently initiator terminated chains should be only in the range of 5% for each step. The detailed reaction conditions for the various polymers are summarized in Table 1.

According to the generally accepted mechanism of the RAFT process,[6,76] the polymers inevitably lose a small portion of the active thiocarbonyl end goups ("Z-group") after each polymerization step. While this can be easily neglected for well-conducted reactions in the case of homopolymers, this feature of polymers made by the RAFT method becomes increasingly problematic with the number of sequential polymerizations performed and when the polymers produced are to be used as macro-RAFT agents in a subsequent polymerization. Such polymer intermediates are mostly characterized by size exclusion chromatography (SEC), though SEC is limited to information about the (often only apparent) molar masses and molar mass distributions. Because of the lack of practical alternatives, relatively low polydispersities (PDI < 1.2−1.4) are then taken as indication for a well-controlled RAFT polymerization resulting in macro-RAFT agents with a high end-group functionality. However, this indicator is only of limited value because a possible loss of active Z-groups in the late stage of the polymerization process would not necessarily affect the polydispersity notably. Apart from this fundamental shortcoming, the use of the polydispersity as quality indicator of macro-RAFT agents is hampered by the widespread difficulty to characterize amphiphilic block copolymers by meaningful SEC analysis, as they often do not fulfill the prerequisits, such as being molecularly dispersed in the eluent while not interacting with the column material. Moreover, pertinent calibration standards to deduce absolute molar masses are generally not available. This problem is particularly present for triphilic block copolymers due to their often complex mutual interactions[13,22] as well as their disparate affinities for solvents and column materials. To overcome this analytical problem, we recently conceived new RAFT agents bearing two complementary end-group labels that can be easily and independently quantified by ^{1}H NMR. This strategy enables to analyze not only the absolute molar masses of the polymers produced but also the extent of end-group functionality.[74] Such a double-labeled RAFT agent bearing two discernible trimethylsilyl (TMS) labels, namely CTA 4-(trimethylsilyl)benzyl 4′-(trimethylsilyl)butane dithioate, was employed for the synthesis of the new triphilic block copolymers. Thus, neglecting the small share of inherently initiator terminated polymer chains, absolute molar masses of the polymers could be determined—whereas attempts for meaningful SEC analysis of the block copolymers

failed—and the preservation of the Z end groups verified after each polymerization step.

Accordingly, the isolated polymers were characterized by ^{1}H NMR (Table 2), as illustrated in Figure 2. After purification by dialysis, the polymers were free of residual monomer. The signals attributed to the ester methylene protons −COO−CH_2− of the three repeat units derived from monomers OEGA, BzA, and FA (at δ = 4.17, 4.92, and 4.55 ppm, respectively) are well resolved. Beyond confirming the presence of all three monomers in the various copolymers qualitatively, these signals also enabled their quantification relative to each other as well as relative to the signal of the TMS label of the R-group at 0.25 ppm and to the signal of the complementary TMS label of the Z-group at 0 ppm. Furthermore, ^{19}F NMR spectra verified the presence of fluorocarbon units in the copolymers containing a fluorophilic block (cf. Supporting Information). Thus, copolymer compositions, absolute number-average molar masses, and the contents of active Z-groups could be determined.

The compiled analytical data (Table 2) demonstrate that the triphilic block copolymers with all permutated sequences of the hydrophilic, lipophilic, and fluorophilic blocks (ABC, ACB, and BAC, cf. Figure 1) were successfully prepared from the respective monomers, using three successive RAFT polymerizations. The M_n values derived from the analysis of the R-groups agree very well with those theoretically calculated (M_n^{theo}) for the homopolymers as well as the various block copolymers, indicating a well-controlled polymerization process. If the reactions are appropriately conducted, the block copolymers contain high contents of RAFT active end groups even after all three polymerization steps (≥80%, see Table 2, entries 15−17). Still, it becomes also clear that high end-group functionalities cannot be implied a priori, in particular for block copolymers. This is exemplified by {$OEGA_{70}$-FA_{10}} or {BzA_{45}-FA_{60}} (entries 5 and 7 in Table 2), in which about 1 out of 3 polymers lost its RAFT active Z-group. Hence, we refrained from their use as macro-RAFT agents, which would have resulted in triblock copolymers with a high content of diblock copolymer contaminants.

M_n values could be also estimated from analyzing the content of the thiocarbonyl moiety of the Z-group by UV spectroscopy.[77−81] The derived M_n(UV) values are generally in reasonable agreement with the corresponding values of M_n^{theo}, corroborating the NMR results. This finding seems also important in a larger context, as trithiocarbonates and dithioesters inherently contain this chromophore. This enables the convenient estimation of M_n without the need of particular labeling efforts, in particular in the case of homopolymers (see Table 1, entries 1−3). Still, a closer look at the data reveals that M_n(UV) tends to overestimate the absolute values. The discrepancy increases for the diblock and even more the triblock copolymers within a given sequence of polymerizations (compare e.g. in Table 2 entry 1 with entries 4−5 and entries 8−9, entry 2 with entries 14 and 17, or entry 11 with entries 12−13 and entries 15−16). This is consistent with the partial loss of Z-groups expected theoretically and as seen in the ^{1}H NMR spectra. In fact, when correcting the M_n(UV) values for this loss, the resulting values M_n*(UV) coincide remarkably well with the values of M_n obtained from ^{1}H NMR and with M_n^{theo}.

DSC measurements of the polymers showed only glass transitions in the thermograms, but no melting events. Glass transitions were found at about −65 °C for the polyOEGA block, at about −24 °C for the polyBzA block, and at about −27 °C for the polyFA block. Accordingly, the polymers are amorphous, and not "frozen" at the temperatures of liquid water. Copolymers with a polyOEGA block always exhibited two glass transitions, indicating microphase separation of the hydrophilic and the hydrophobic blocks already in the bulk. However, the close proximity of the glass transitions of the lipophilic and fluorophilic blocks precluded from judging the solid state (in)compatibility of the different hydrophobic blocks by DSC.

Table 3. Hydrodynamic Diameters D_h and Polydispersities PD of the Aggregates of Homopolymer, Diblock Copolymers, and Triblock Copolymers in 0.5 wt % Aqueous Solution, Obtained from DLS Measurements, before Thermal Treatment

entry	polymer	D_h [nm]	PD
1	{$OEGA_{70}$}	6	0.04
2	{$OEGA_{70}$-BzA_{20}}	110	0.11
3	{$OEGA_{70}$-FA_{10}}	90	0.05
4	{BzA_{45}-$OEGA_{175}$}	135	0.08
5	{$OEGA_{70}$-BzA_{20}-FA_{35}}	100	0.09
6	{$OEGA_{70}$-FA_{10}-BzA_{25}}	150	0.07
7	{BzA_{45}-$OEGA_{175}$-FA_{40}}	140	0.08
8	{$OEGA_{40}$-BzA_{45}-FA_{30}}	70	0.02
9	{$OEGA_{40}$-FA_{30}-BzA_{45}}	200	0.15
10	{BzA_{45}-$OEGA_{40}$-FA_{30}}	85	0.03

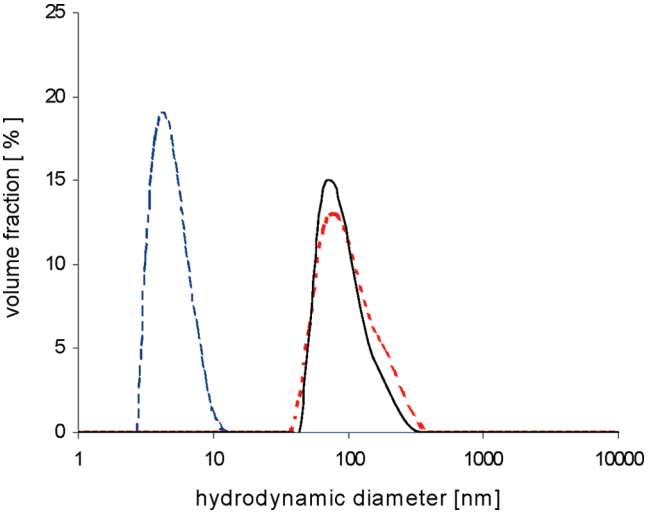

Figure 3. Comparison of particle size distributions obtained by DLS in 0.5 wt % aqueous solution of homopolymer (---), diblock (···), and triblock (—) copolymers before annealing.

Aggregation Behavior of the Block Copolymers in Water. Aqueous dispersions of the polymers were studied by dynamic light scattering (DLS). Analysis of solutions of homopolymer polyOEGA disclosed only very small structures with mean hydrodynamic diameters (D_h) below 10 nm. This size corresponds to molecularly dissolved coils of polyOEGA polymers. DLS analysis of the di- and triblocks revealed the presence of colloids with mean D_h values in the range of 90 to 150 nm (Table 3, Figure 3). The differences between the diblock and corresponding triblock copolymers concerning the size or size distribution are small. Apparently, possible differences in the micellar core have little influence on the hydrodynamic diameter. The size distributions appear monomodal at first sight, but in most cases, a shoulder points to a small population of bigger

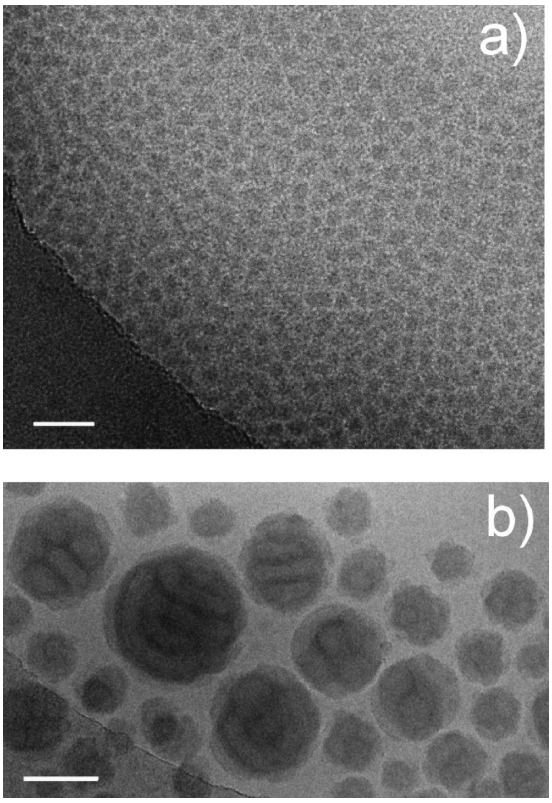

Figure 4. Cryo-TEM images of a 0.5 wt % solution of poly{BzA_{45}-$OEGA_{40}$-FA_{30}} in water: (a) as prepared at ambient temperature (scale bar: 50 nm); (b) after annealing for 2 weeks at 75 °C (scale bar: 50 nm).

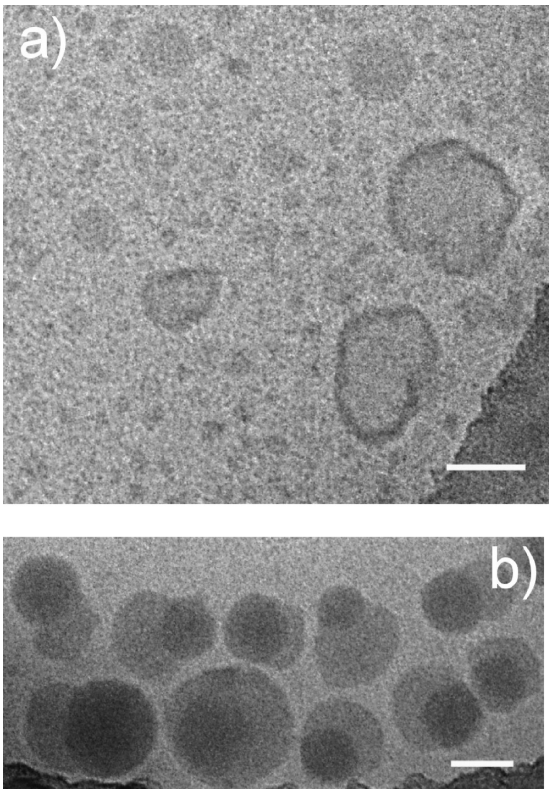

Figure 5. Cryo-TEM images of a 0.5 wt % solution of poly{BzA_{45}-$OEGA_{175}$-FA_{40}} in water: (a) as prepared at ambient temperature; (b) after annealing for 2 weeks at 75 °C. Scale bars: 50 nm.

aggregates in the 150−300 nm range. As DLS provides no information about the geometry, the bigger aggregates might be for instance micelle clusters.

Different from scattering methods such as DLS, which provide averaged particle sizes and size distributions for the self-assembled aggregates of the triblock copolymers, cryo-TEM visualizes the individual micelles directly.[20,28,33−37,40−45,82] Hence, quantitative data characterizing the micellar aggregates' overall dimensions, their morphology and ultrastructure, i.e. the size and distribution of segregated nano domains, can be obtained.

All block sequences—ABC, ACB, and BAC—were investigated (Figures 4−9). For each block sequence, two polymer samples with different block lengths were studied, revealing that differing block sequences as well as differing relative block sizes will influence the micellar structures. In the first series of copolymers with permutated block sequences, the hydrophilic polyOEGA block (A) had a share of about 50 wt % (Table 2, entries 15−17), while in the second series, the share of polyOEGA block was between 70 and 85 wt % (Table 2, entries 8−10). Also, the relative masses of the lipophilic (B) and fluorophilic (C) blocks in the first series were about the same, with mass fractions of about 0.25 each. While in the second series the mass fraction of the B block was fixed to about 0.1, the mass fraction of the C block was about 0.2, 0.1, and 0.1 for the sequences ABC, BAC, and ACB, respectively.

A typical observation in the cryo-TEM images is that fluorocarbon domains provide much higher contrast compared to hydrocarbon domains. This fact is due a high electron density of fluorine derivatives[33] and therefore allows the domains to be easily differentiated in the images. The well-hydrated domains of the hydrophilic polyOEGA block remain generally invisible since their electron density coincides with that of vitrified water layer in which the particles are embedded.

We noted quite frequently in the cryo-TEM images of the different systems we studied that smaller and larger spherical aggregates with core diameters ranging from 20 to 200 nm coexist and that the polydispersity decreases upon annealing of the samples (2 weeks at 75 °C). When broad size distributions are observed initially, the share of smaller aggregates is significantly reduced upon annealing. This is qualitatively in agreement with the DLS results. An evolution of the size of colloidal objects has been often reported in aqueous solutions of amphiphilic block copolymers.[20,44,83−86] A surprising finding was that in some cases the size of aggregates did not decrease upon annealing as well documented recently for instance for PB−PEO block copolymer micelles[87] but increased instead. It remains an open question whether all the different structures are equilibrium structures or not and to which extent the polydispersity of the block copolymers contributes to the size distributions. In any case, kinetic effects in the preparation and aging of such block copolymer aggregates are most probable,[40,88−91] even if all blocks display a low glass transition temperature as in our case.

A previous study with linear triphilic ternary block copolymers revealed that the block sequence BAC was best suited to form multicompartment micelles, whereas the block sequence ABC rather induced the formation of core−shell−corona micelles.[44] Therefore, copolymers of the BAC type were investigated first. Typical cryo-TEM images of micellar solutions of polymer poly{BzA_{45}-$OEGA_{40}$-FA_{30}} are depicted in Figure 4 before

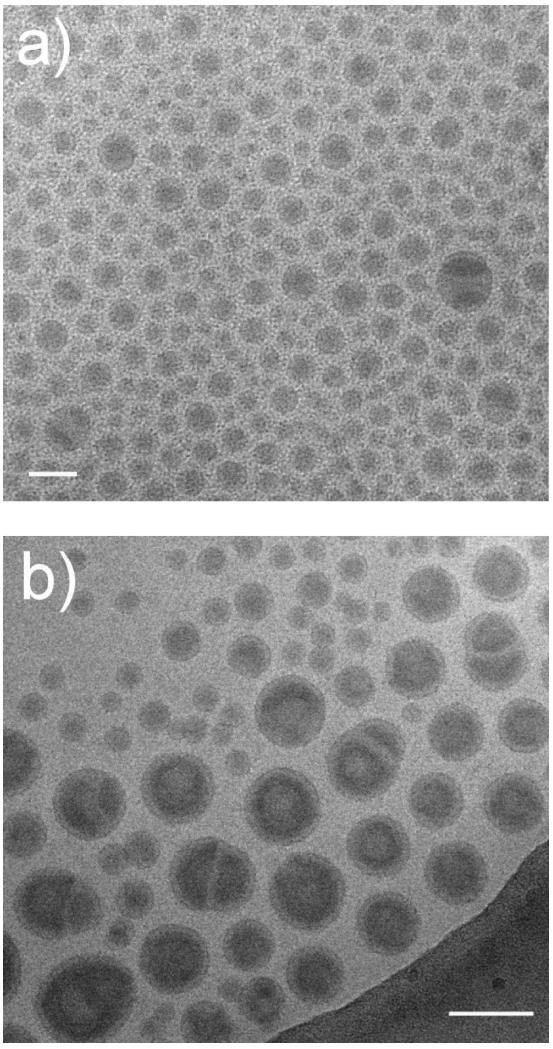

Figure 6. Cryo-TEM images of a 0.5 wt % solution of poly{$OEGA_{40}$-BzA_{45}-FA_{30}} in water: (a) as prepared at ambient temperature (scale bar: 50 nm); (b) after annealing for 2 weeks at 75 °C (scale bar: 100 nm).

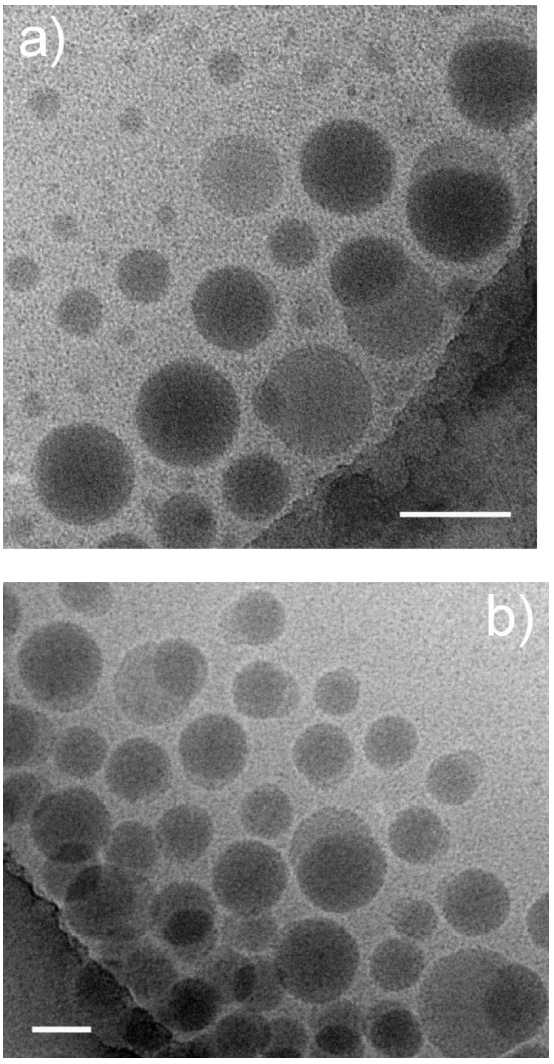

Figure 7. Cryo-TEM images of a 0.5 wt % solution of poly{$OEGA_{70}$-BzA_{20}-FA_{35}} in water: (a) as prepared at ambient temperature (scale bar: 50 nm); (b) after annealing for 2 weeks at 75 °C (scale bar: 100 nm).

and after an annealing treatment for 2 weeks at 75 °C. At first the copolymer self-assembles into very small monodiperse micelles with a core diameter below 20 nm (Figure 4a). A microphase separation within the micellar core cannot be detected. After annealing, the small micelles are replaced by bigger aggregates with typical core diameters in the range of 50−100 nm. The formation of subdomains within the core (Figure 4b) with high contrast can be observed. Dark fluorinated domains (F) seem to form "walls" with a thickness of about 10 nm that separate multiple cell-like hydrocarbon domains (H) inside the core each having a width of about 20 nm. In the case of the smaller aggregates, the "cells" seem to possess a spherical shape, while for the largest aggregates, they appear to be cylindrical. Obviously, the short perfluoropropyl residue on the polyacrylate backbone suffices to induce a microphase separation within micellar aggregates. The packing structure of the large aggregates can be explained by a periodic stacking of "...-HFFH-HFFH-..." domains. The estimated "wall" (F) and "cell" (H) dimensions are not larger than twice the contour lengths of the fluorinated and hydrocarbon blocks $L^F \approx 7.5$ nm and $L^H \approx 11$ nm, respectively, and thus are consistent with the molecular dimensions. The hydrophilic segments ($L^O \approx 10$ nm) should form loops outside of the core going from one "cell" to the next "wall", as sketched in Scheme 1.

In fact, the dimension of a cell cannot be larger than twice the length of a hydrophilic loop. However, for large spherical aggregates, some fraction of the hydrophilic blocks must be assumed to be incorporated into the interior of the hydrophobic micellar core.[41,62] Because cryo-TEM provides only a 2D projection of 3D objects, it is not possible to decide whether the large aggregates are spherical or disklike. To offer evidence, we attempted cryo electron tomography (cryo-ET)[41] but failed because of the high radiation sensitivity of samples, resulting in the fast destruction of the aggregates while taking a tilt series. Therefore, we restricted our observation to stereo image pairs, which allow for a three-dimensional observation of the structures. These investigations confirmed that the large aggregates are most probably spherical structures. A representative stereo image is shown in Figure S1. Figure 5 presents typical cryo-TEM images of micellar solutions of the analogous BAC block copolymer with a larger polyOEGA block, namely poly{BzA_{45}-$OEGA_{175}$-PFA_{40}}, prepared before and after the annealing procedure. The polymer prepared at ambient temperature forms

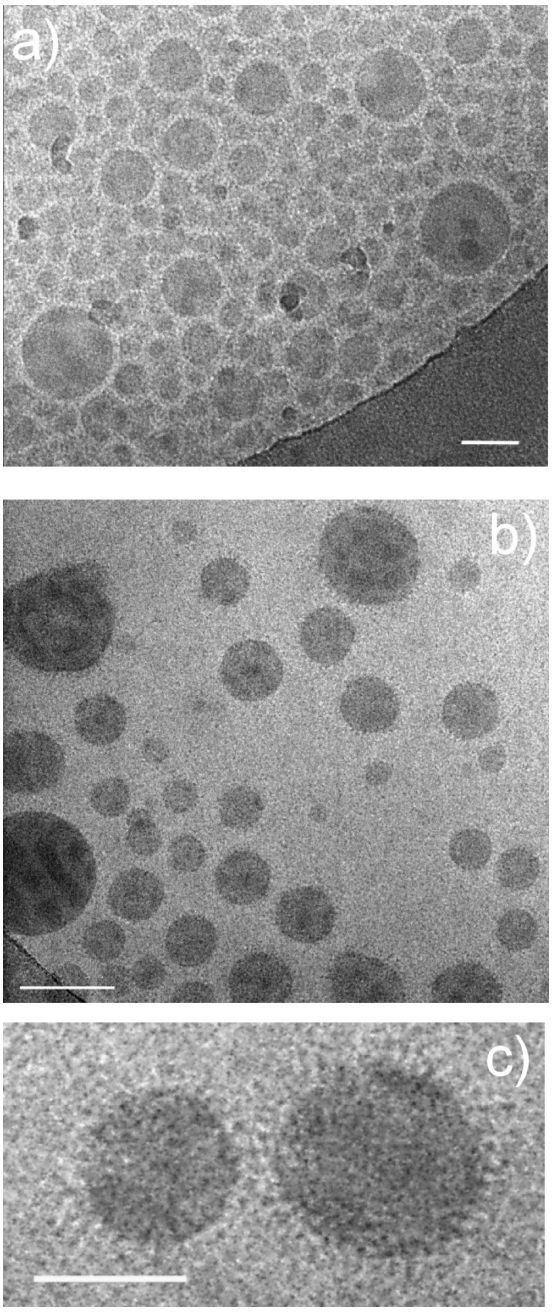

Figure 8. Cryo-TEM images of a 0.5 wt % solution of poly{$OEGA_{40}$-FA_{30}-BzA_{45}} in water: (a) as prepared at ambient temperature; (b) after annealing for 2 weeks at 75 °C. (c) At high magnification the corona can be discerned as a fringed seam surrounding the micellar core. Scale bars: 50 nm.

small spherical micelles and only few larger aggregates, some of which show a vesicle-like density profile (Figure 5a). Again, microphase separation cannot be detected in fresh solutions. The vesicle-like structures have a characteristic electron dense membrane. The polyFA and polyBzA blocks are probably both present in the membrane. Still, any local microphase separation, if occurring at all, is not large enough to form distinguishable domains. After annealing, both the small micelles and the vesicles disappear (Figure 5b). They were replaced by bispherical structures made of one dark and one bright approximately spherical subdomain. According to the contrast conditions, these

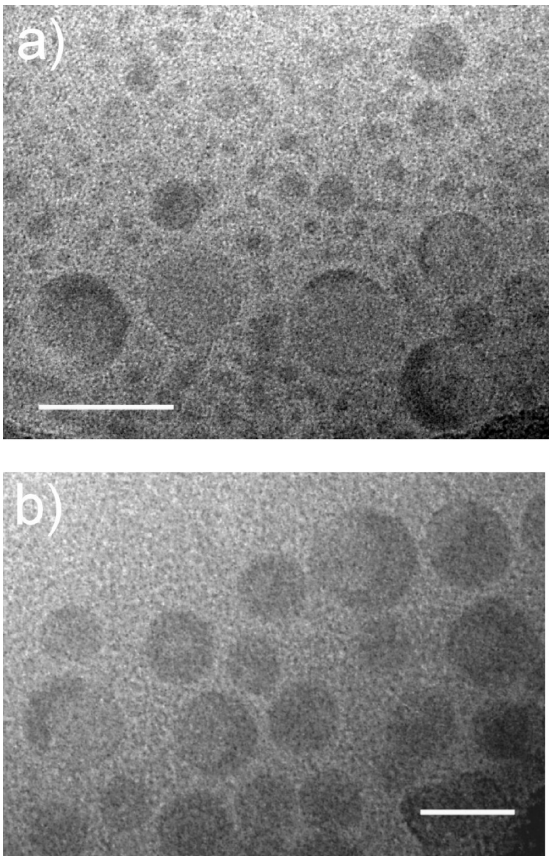

Figure 9. Cryo-TEM images of a 0.5 wt % solution of poly{$OEGA_{70}$-FA_{10}-BzA_{25}} in water: (a) as prepared at ambient temperature (scale bar: 50 nm); (b) after annealing for 2 weeks at 75 °C (scale bar: 100 nm).

correspond to the fluorophilic fluorocarbon containing and the lipophilic hydrocarbon compartments, respectively. Note that the latter domains are partly overlapped by the darker fluorocarbon domains, as the bispherical micelles can adopt various orientations in the sample. Most interestingly, the shape of the bispherical structure corresponds to a multicompartment micelle as has been theoretically predicted by de Gennes about 10 years ago.[52] Still, if one compares the sizes of the hydrophobic domains with the respective block lengths, the domains' diameters are considerably larger than the constituting block lengths of about 10 nm, the reasons of which are unclear yet.

One may speculate why in the case of the much shorter hydrophilic A block of the BAC block sequence bispherical structures were not observed in fresh samples (cf. Figure 4a). Possibly, the totally different morphology of poly{BzA_{45}-$OEGA_{40}$-FA_{30}} results from the clustering of multiple core−shell−corona micelles, so that fluorinated shells become walls within the growing aggregates.

Figures 6 and 7 illustrate typical cryo-TEM images of micellar solution of polymers with the ABC sequence hydrophilic−lipophilic−fluorophilic blocks, namely of {$OEGA_{40}$-BzA_{45}-FA_{30}} and {$OEGA_{70}$-BzA_{20}-FA_{35}}. Again, images were taken before and after annealing the samples for 2 weeks at 75 °C. Block copolymer poly{$OEGA_{40}$-BzA_{45}-FA_{30}} self-assembled into core−shell−corona micelles, with the dark fluorinated domain in the center surrounded by a hydrocarbon shell, shielding the inner hydrophobic core from the aqueous environment (Figure 6a). The size distribution is narrow and the mean

size of the micelles is quite small, exhibiting an hydrophobic domain diameter in the range of 20−40 nm. The observed core−shell−corona ultrastructure agrees very well with the findings of a previous study of analogous ABC triblock copolymers (yet with a much longer perfluoroctyl fluorocarbon side chain).[44] After annealing, bigger aggregates appear (Figure 6b, cf. also Figure S2), which show unusually shaped fluorinated domains. Their shape might be described as capsules (one or two) made of polyFA located in the interior of the micellar core and separated from the water interface by a shell of polyBzA. Even when two capsules are present, they do not contact each other (for a corresponding cryo-TEM red-cyan anaglyph, cf. Figure S3). Some small core−shell−corona micelles are still present in addition to the bigger aggregates. Maybe, the structural reorganization is not yet complete. Still, it is impossible to say whether the new, bigger structures are thermodynamically more favorable or whether the colloidal growth results from insufficient stabilization by the hydrophilic corona.

To our surprise, the analogous ABC block copolymer {$OEGA_{70}$-BzA_{20}-FA_{35}}, with the higher share of polyOEGA block, did not self-assemble into core−shell−corona structures, but formed multicompartment micelles instead. Bispherical, bipolar structures with dark spheres of fluorinated domains, and brighter spheres of less electron-dense hydrocarbon domains are visible (Figure 7), which are very similar to those found for the BAC type poly{BzA_{45}-$OEGA_{175}$-PFA_{40}}. The broad size distribution of the micelles is narrowed by annealing, making the smaller micelles of the initial population disappear. Probably, the smallest micelles merge with others to give a population with typically 50 nm mean core size. The volume of the fluorinated domains seems predominant compared to those of the polyBzA block, which is in agreement with the relative high share of polyFA in this sample. Note that the hydrocarbon domains are partly obscured by the darker fluorocarbon domains, as the bispherical micelles can adopt various orientations in the sample. Concerning the overall dimensions, aggregates of 60 nm core diameter and above are difficult to explain taking the lengths of the hydrophobic copolymer blocks into account. The total contour length of the polymers is ∼32 nm. The contour length of the cumulated hydrophobic segments is about 15 nm only, and the polymers are certainly not in their fully extended conformation. Therefore, the ultrastructures may be more complex than a simple bispherical core with complete segregation of the immiscible lipophilic and fluorophilic blocks. In fact, highly complex ultrastructures in multicompartment micelles made from ternary block copolymers were reported recently.[41]

The differences between the micellar structures of the two block copolymers (Figures 6 and 7) made of the same monomers and having the same block sequence ABC is remarkable. Both the increased length of the hydrophilic block and the increased relative share of the fluorophilic block in comparison to the lipophilic block may contribute to the differences. The resulting enhanced curvature of the overall hydrophobic domain as well as the increased volume need of the fluorophilic block should favor deviations from a core−shell−corona ultrastructure, thus facilitating the formation of multicompartment micelles.

The aqueous self-assembly of triphilic block copolymers with the block sequence hydrophilic−fluorophilic−lipophilic ACB has not been investigated before. Typical cryo-TEM images of micellar solution of polymers poly{$OEGA_{40}$-FA_{30}-BzA_{45}} and poly{$OEGA_{70}$-FA_{10}-BzA_{25}} are displayed in Figures 8 and 9, before and after annealing.

Scheme 1. Schematic Model of an Aggregate Formed by Poly{BzA_{45}-$OEGA_{40}$-FA_{30}} in Water after the Annealing Procedure[a]

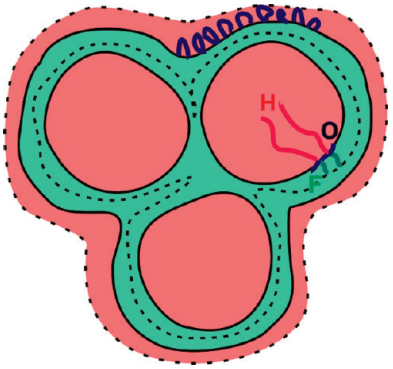

[a] Fluorinated domains (F) form "walls" that separate multiple cell-like hydrocarbon domains (H). The hydrophilic block (O) forms loops outside of the core and stabilizes the aggregates. A certain fraction of the hydrophilic segments is incorporated into the interior of the hydrophobic core at the interface between the hydrocarbon and the fluorinated domains. Red, green, and blue represent the H, F, and O blocks, respectively.

Polymer poly{$OEGA_{40}$-FA_{30}-BzA_{45}} forms spherical, compartmentalized micelles (Figure 8, cf. also Figure S4) reminiscent of soccer balls. The micelle size distribution was broad before the annealing treatment. However, in accordance with the other cases, the aggregate size increases at the expense of smaller aggregates upon annealing. The dark fluorinated domains appear as small disks on the surface of the lipophilic micellar core. Such mutual arrangement could be expected as the fluorinated block is tethered to the corona-forming hydrophilic block here. However, fluorinated domains might also be embedded within the lipophilic core, as a recent study of morphologically quite similar micelles formed by another triphilic block copolymer with BAC block has shown.[44] In that case, it was possible to demonstrate by using cryo-ET[41] that the fluorinated domains were located at the surface as well as deeply within the lipophilic core of the aggregates. Figure 8c shows two micelles at high magnification. Here the corona can be discerned as a fringed seam surrounding the micellar core. We attribute this to the compact bottle brush-like conformation of the $OEGA_{40}$ block, which appears with high contrast.[41] The thickness of the fringed corona is between 5 and 10 nm and thus consistent with the contour length of the hydrophobic block of about 11 nm. In the case that the micelles are closely packed as exemplary shown in Figure 8a, the thickness of the corona can as well be estimated from the micelles' smallest distance to the neighbors. Both estimates well agree.

Polymer poly{$OEGA_{70}$-FA_{10}-BzA_{25}} forms spherical micelles, too (Figure 9), with a broad size distribution, which is, again, narrowed by annealing. As for the ACB analogue—disposing of a shorter A and a longer C block—described above, a multicompartment structure is formed. Here, the dark fluorinated domains appear to form incomplete shells at the interface between the hydrophobic micellar core and the hydrophilic corona. This shape might be explained by the rather short polyFA segment ({FA_{10}} only) and the corresponding small volume of the fluorinated nanodomain. The position of this domain at the interface with the corona may be considered as a consequence of the direct covalent linkage of the fluorophilic to the hydrophilic block.

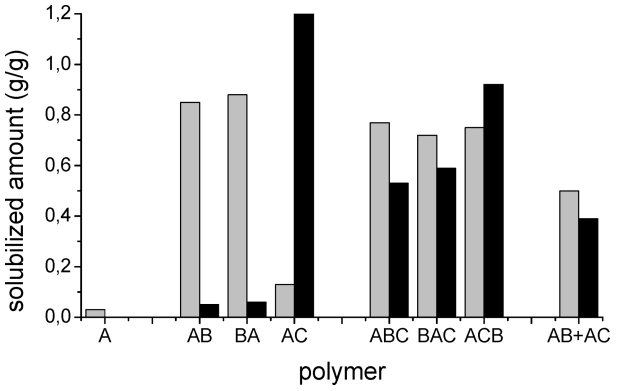

Figure 10. Solubilization of neopentylbenzene (gray bars) and hexafluorobenzene (black bars) by 0.3 wt % aqueous solutions of amphiphilic diblock and triblock copolymers. A represents the hydrophilic block $OEGA_{40}$, B the lipophilic block BzA_{45}, and C the fluorophilic block FA_{30}.

The micellar structure of the block copolymers with the sequence ACB show some common features. In both cases, the fluorinated domains do not form complete shells, but unique sickle-shaped domains are formed at the interface in the case of poly{$OEGA_{70}$-FA_{10}-BzA_{25}} and structurally similar microphase disks in the case of poly{$OEGA_{40}$-FA_{30}-BzA_{45}}. As emphasized above, however, it cannot be excluded that some fluorinated domains are also present in the center of the core. But such domains are less probable because the polyFA blocks are covalently attached to the hydrophilic polyOEGA block forming the corona.

The structural differences between the sickle shape and the soccer ball shape of the fluorinated domains may be a consequence of the differing lengths of the polyFA blocks. While polyFA had about 40% of the length of the polyBzA block in the first ACB-type, poly{$OEGA_{70}$-FA_{10}-BzA_{25}}, it had about 70% of it in the second case, poly{$OEGA_{40}$-FA_{30}-BzA_{45}}. The resulting volume ratios may explain why the fluorophilic domains occupy a larger fraction of the interface.

Summarizing the observations obtained by cryo-TEM, it becomes clear that not only the block sequence but also the relative lengths of the blocks are important parameters for the self-assembly of the triphilic block copolymers in selective solvents. Nevertheless, the influence of the block sequence seems particularly important. Further, kinetic effects must be taken into account. The comparison underlines that the self-assembly of triblock copolymers in selective solvents can be tuned by a number of molecular parameters and that various multicompartment ultrastructures are possible.

Selective Solubilization by the Block Copolymer Micelles. Having established the formation of micellar aggregates with multicompartment ultrastructures, solubilization of hydrocarbon and fluorocarbon guest molecules by the various micellar systems was investigated with respect to their selective uptake in compartments. The aromatic hydrophobic liquids neopentylbenzene (NPB) and hexafluorobenzene (HFB) were employed as lipophilic and as fluorophilic guests. These solubilizates were chosen, as they can be easily identified and quantified by ^{1}H and ^{19}F NMR spectroscopy, respectively, and their characteristic singlet signals are well resolved from the polymer signals in the spectra. Further, both solubilizates are virtually insoluble in water in the absence of polymer. Hence, their marginal amounts dissolved in the aqueous matrix can be neglected to the amounts solubilized in the hydrophobic cores of the polymer micelles.

Table 4. Solubilization Efficiencies of the Polymeric Micelles for Neopentylbenzene (NPB) and Hexafluorobenzene (HFB)[a]

	block sequence						
mass ratio considered	AB	BA	AC	ABC	BAC	ACB	mixture of AB + AC
NPB/B	0.50	0.52		0.59	0.55	0.57	0.56
NPB/(B + C)	0.50	0.52	0.07	0.29	0.27	0.28	
HFB/C			0.69	0.40	0.44	0.70	0.65
HFB/(B + C)	0	0	0.69	0.20	0.22	0.34	

[a] Mass ratios of solubilized compound compared to the mass of the lipophilic, fluorophilic, and all hydrophobic (lipophilic and fluorophilic) blocks, respectively, of the copolymers in the compartmented aggregates. A represent the hydrophilic block $PEGA_{40}$, B the lipophilic block $PBzA_{45}$, and C the fluorophilic block PFA_{30}.

Solubilization experiments were carried out for a set of polyOEGA homo-, diblock, and triblock copolymers, using samples with a similar size of the A, B, and C blocks (Table 2, entries 11−17). Reference samples of pure D_2O were checked to confirm the virtual insolubility of NPB and HFB in water. The results are presented in Figure 10 and Table 4.

The capacity of the homopolymer polyOEGA (block A) to solubilize NPB dissolved in D_2O is marginal, i.e., close to the value of the pure solvent, indicating a very low affinity of the lipophobic compound for the hydrophilic block. In contrast, when polyBzA blocks (block B) are present, the solubility of NPB in the systems increases strongly. Remarkably, when the polyBzA block is replaced by polyFA (block C) as in the case of poly{OEGA-*b*-FA} diblock system, the amount of solubilized NPB is much smaller than for their poly{OEGA-*b*-BzA} analogues. Comparing diblock and triblock copolymer systems, the amount of NPB solubilized by the triblock copolymer micelles is still high but is slightly reduced in comparison to poly{OEGA-*b*-BzA} diblock micelles (Figure 10). This is a result of the reduced mass of polyBzA in the hydrophobic core of the triblock copolymer micelles (cf. Table 4). The effect is even more pronounced when physical mixture of diblock copolymers AB + AC is used (Table 4), as the share of hydrophilic blocks needed to stabilize the mixed micelles is markedly higher than in the triblock copolymers.

Looking at the solubilization of the fluorocarbon probe, the capacity of polyOEGA to solubilize HFB dissolved in D_2O is marginal, i.e., close to the value of the pure solvent, indicating a very low affinity of the fluorophilic compound for the hydrophilic block, too. In analogy to the solubilization of the lipophilic probe NPB by the lipophilic polyBzA block, the solubility of HFB in the systems increases strongly when polyFA blocks are present. Again, when the polyFA block is replaced by polyBzA as in the case of the poly{OEGA-*b*-BzA} diblock system, the amount of solubilized HFB is reduced to a very small value in comparison. Also when comparing diblock and triblock copolymer systems, the amount of HFB solubilized by the triblock copolymer micelles is still high, but somewhat lower than in the case of the poly{OEGA-*b*-FA} diblock micelles (Figure 10). This is due to the reduced mass of polyFA in the hydrophobic core of the triblock copolymer micelles.

These findings demonstrate that, on the one hand, the block copolymer micelles have a high capacity to solubilize aromatic hydrophobic compounds. Moreover, the various systems studied show a marked selectivity concerning the solubilizate uptake. While the lipophilic compound NPB is efficiently accommodated only in polymer micelles containing a lipophilic polyBzA block, the analogous effect is observed for the fluorophilic compound HFB in polymer micelles containing a fluorophilic polyFA block. The simultaneous solubilization of both NPB and HFB requires either the use of the triblock copolymers or of a physical mixture of diblock copolymers. If the corresponding block is missing, the uptake of the hydrophobic probes becomes very small. Accordingly, the lipophilic and fluorophilic compartments in the micelles are capable of selective solubilization. The selectivity is significant, in particular in the case of the fluorocarbons, though not 100%.

In order to better judge the solubilization selectivity, the amounts of solubilized material (Figure 10) can be normalized to the hydrophobic (blocks B + C, lipophilic (i.e., polyBzA, block B) or fluorophilic (i.e., polyFA, block C) mass fraction in the micellar core (Table 4). In the case of the lipophilic probe NPB, the solubilized amounts normalized to the polyBzA content are very similar for the various diblock and the triblock copolymers, independent of the block sequence. A comparable value is found for a physical mixture of the AB and AC diblock copolymers, too. There seems to be a slight advantage for the triblock copolymers in comparison to the diblock copolymers due to the small, but not negligible, contribution of the polyFA block to the solubilization of NPB. From the data in Table 4, one can derive that the share of lipophilic probe solubilized in the lipophilic polymer domains is in the range of 80−90%, while the share of fluorophilic probe solubilized in the fluorophilic polymer domains is well above 95%.

In the case of the fluorophilic probe HFB, the solubilized amounts normalized to the polyFA content are very similar for the diblock and triblock copolymer with the sequence ACB, but to the same extent smaller for the triblock copolymers with the sequences ABC and BAC. Obviously, the solubilization of HFB is hardly supported by the additional presence of polyBzA blocks, but the ultrastructure of the polyFA domains in the micelles seem to play a role. Considering the distinct morphologies observed by cryo-TEM, it is not surprising that differences between micelles made from triblock copolymers with different block sequence occur. Still, the effects are difficult to rationalize at present. For the lipophilic solubilizate, the block sequence apparently does not to affect the solubilization capacity; i.e., the different micellar morphologies and ultrastructures seem to be not important.

CONCLUSIONS

New linear triphilic block terpolymers, with hydrophilic (poly(oligoethylene glycol acrylate), A), lipophilic (poly(benzyl acrylate), B), and fluorophilic (poly(heptafluorobutyl acrylate), C) blocks, were synthesized with various block lengths and all permutations of block sequences ABC, BAC, and ACB, the latter being investigated for the first time. Using the RAFT process, analysis of the molar masses was made possible by an R- and Z-group labeled RAFT agent, providing two different trimethylsilyl moieties for end-group analysis by NMR. Dynamic light scattering studies confirmed the formation of micellar aggregates by the copolymers in water. Cryo-TEM imaging enabled the visualization of multiple morphologies in the micelles populations: core−shell−corona micelles, spherical micelles with "sickle" fluorocarbon domains at the external interface of the core, bispherical micelles, "soccer ball" morphologies, micelles with "capsule" fluorocarbon domains inside the core, micelles with "cell" morphologies and vesicles. Bispherical micelles, as were theoretically predicted by de Gennes for the structure of multicompartment micelles, were found for the first time. The lengths of the individual blocks in the copolymers as well as the block sequences strongly influence the micellar morphologies, but annealing treatments also have a significant effect.

Solubilization experiments probed the potential of the new multicompartment micelles with respect to the selective uptake of specific hydrophobic molecules, using the model guest compounds neopentylbenzene and hexafluorobenzene. Highly selective solubilization by the multicompartment systems was observed, in particular for fluorocarbons. As the different micellar morphologies show similar solubilization capacities, geometrical effects seem to be of secondary importance. Solubilization is apparently mostly influenced by the volume fraction of the core subdomain that is compatible with the guest molecule.

ASSOCIATED CONTENT

Supporting Information. Stereo images of poly{BzA_{45}-$OEGA_{40}$-FA_{30}} and poly{$OEGA_{40}$-BzA_{45}-FA_{30}} micelles and additional cryo-TEM micrographs of aqueous solutions of poly{$OEGA_{40}$-BzA_{45}-FA_{30}} and poly{$OEGA_{40}$-FA_{30}-BzA_{45})} after annealing; ^{19}F NMR spectra of copolymer poly{$OEGA_{70}$-*b*-FA_{10}}. This material is available free of charge via the Internet at http://pubs.acs.org.

AUTHOR INFORMATION

Corresponding Author

*A.L.: Tel +49 331 977 5225, Fax +49 331 977 5036, e-mail laschews@rz.uni-potsdam.de. H.v.B.: Tel +49 30 838 53982, Fax +49 30 838 56589, e-mail h.v.berlepsch@fzem.fu-berlin.de.

ACKNOWLEDGMENT

Financial support was provided by the Deutsche Forschungsgemeinschaft (grants LA611/5 and BO1000/8).

REFERENCES

(1) Förster, S.; Plantenberg, T. *Angew. Chem., Int. Ed.* **2002**, *41*, 688–714.
(2) Antonietti, M.; Förster, S. *Adv. Mater.* **2003**, *15*, 1323–1333.
(3) Hamley, I. W. *Block Copolymers in Solution: Fundamentals and Applications*; John Wiley & Sons Ltd.: Chichester, England, 2005.
(4) Cohen Stuart, M. A. *Colloid Polym. Sci.* **2008**, *286*, 855–864.
(5) Blanazs, A.; Armes, S. P.; Ryan, A. J. *Macromol. Rapid Commun.* **2009**, *30*, 267–277.
(6) Moad, G.; Rizzardo, E.; Thang, S. H. *Acc. Chem. Res.* **2008**, *41*, 1133–1142.
(7) Matyjaszewski, K.; Müller, A. H. E. *Controlled and Living Polymerizations. From Mechanisms to Applications*; Wiley-VCH: Weinheim, 2009.
(8) Lutz, J.-F. *Polym. Chem.* **2010**, *1*, 55–62.
(9) Le Droumaget, B.; Nicolas, J. *Polym. Chem.* **2010**, *1*, 563–598.
(10) Ishizone, T.; Sugiyama, K.; Sakano, Y.; Mori, H.; Hirao, A.; Nakahama, S. *Polym. J. Jpn.* **1999**, *31*, 983–988.

(11) Triftaridou, A. I.; Vamvakaki, M.; Patrickios, C. S. *Polymer* **2002**, *43*, 2921–2926.
(12) Lodge, T. P.; Hillmyer, M. A.; Zhou, Z.; Talmon, Y. *Macromolecules* **2004**, *37*, 6680–6682.
(13) Mertoglu, M.; Garnier, S.; Laschewsky, A.; Skrabania, K.; Storsberg, J. *Polymer* **2005**, *46*, 7726–7740.
(14) Fustin, C.-A.; Abetz, V.; Gohy, J.-F. *Eur. Phys. J. E* **2005**, *16*, 291–302.
(15) Kubowicz, S.; Baussard, J.-F.; Lutz, J.-F.; Thünemann, A. F.; Berlepsch, H. v.; Laschewsky, A. *Angew. Chem., Int. Ed.* **2005**, *44*, 5262–5265.
(16) Shunmugam, R.; Smith, C. E.; Tew, G. N. *J. Polym. Sci., Part A: Polym. Chem.* **2007**, *45*, 2601–2608.
(17) Hu, J.; Njikang, G.; Liu, G. *Macromolecules* **2008**, *41*, 7993–7999.
(18) Taribagil, R. R.; Hillmyer, M. A.; Lodge, T. P. *Macromolecules* **2009**, *42*, 1796–1800.
(19) Xie, D.; Ye, X.; Ding, Y.; Zhang, G.; Zhao, N.; Wu, K.; Cao, Y.; Zhu, X. X. *Macromolecules* **2009**, *42*, 2715–2720.
(20) Walther, A.; Barner-Kowollik, C.; Müller, A. H. E. *Langmuir* **2010**, *26*, 12237–12246.
(21) Lei, L.; Gohy, J.-F.; Willet, N.; Zhang, J.-X.; Varshney, S.; Jérôme, R. *Macromolecules* **2004**, *37*, 1089–1094.
(22) Skrabania, K.; Kristen, J.; Laschewsky, A.; Akdemir, Ö.; Hoth, A.; Lutz, J.-F. *Langmuir* **2007**, *23*, 84–93.
(23) Stadler, R.; Auschra, C.; Beckmann, J.; Krappe, U.; Voigt-Martin, I.; Leibler, L. *Macromolecules* **1995**, *28*, 3080–3091.
(24) Dormidontova, E. E.; Khokhlov, A. R. *Macromolecules* **1997**, *30*, 1980–1991.
(25) Abetz, V.; Simon, P. F. *Adv. Polym. Sci.* **2005**, *189*, 128–212.
(26) Ringsdorf, H.; Lehmann, P.; Weberskirch, R. Multicompartmentation - a concept for the molecular architecture of life. Book of Abstracts, 217th ACS National Meeting, Anaheim, CA, March 21−25, 1999.
(27) Laschewsky, A. *Curr. Opin. Colloid Interface Sci.* **2003**, *8*, 274–281.
(28) Laschewsky, A.; Marsat, J.-N.; Skrabania, K.; Berlepsch, H. v.; Böttcher, C. *Macromol. Chem. Phys.* **2010**, *211*, 215–221.
(29) Stähler, K.; Selb, J.; Candau, F. *Langmuir* **1999**, *15*, 7565–7576.
(30) Kotzev, A.; Laschewsky, A.; Rakotoaly, R. *Macromol. Chem. Phys.* **2001**, *202*, 3257–3267.
(31) Kotzev, A.; Laschewsky, A.; Adriaensens, P.; Gelan, J. *Macromolecules* **2002**, *35*, 1091–1101.
(32) Candau, F. *Macromol. Symp.* **2002**, *179*, 13–25.
(33) Li, Z.; Kesselman, E.; Talmon, Y.; Hillmyer, M. A.; Lodge, T. P. *Science* **2004**, *306*, 98–101.
(34) Li, Z.; Hillmyer, M. A.; Lodge, T. P. *Langmuir* **2006**, *22*, 9409–9417.
(35) Walther, A.; Müller, A. H. E. *Chem. Commun.* **2009**, 1127–1129.
(36) Liu, C.; Hillmyer, M. A.; Lodge, T. P. *Langmuir* **2009**, *25*, 13718–13725.
(37) Saito, N.; Liu, C.; Lodge, T. P.; Hillmyer, M. A. *ACS Nano* **2010**, *4*, 1907–1912.
(38) Mao, J.; Ni, P.; Mai, Y.; Yan, D. *Langmuir* **2007**, *23*, 5127–5134.
(39) Komenda, T.; Lüdtke, K.; Jordan, R.; Ivanova, R.; Bonné, T.; Papadakis, C. B. *Polym. Prepr. (Am. Chem. Soc., Div. Polym. Chem.)* **2006**, *47* (2), 763–764.
(40) Cui, H.; Chen, Z.; Zhong, S.; Wooley, K. L.; Pochan, D. J. *Science* **2007**, *317*, 647–650.
(41) Berlepsch, H. v.; Böttcher, C.; Skrabania, K.; Laschewsky, A. *Chem. Commun.* **2009**, 2290–2292.
(42) Skrabania, K.; Laschewsky, A.; Berlepsch, H. v.; Böttcher, C. *Langmuir* **2009**, *25*, 7594–7601.
(43) Fang, B.; Walther, A.; Wolf, A.; Yu, Y.; Yuan, J.; Müller, A. H. E. *Angew. Chem., Int. Ed.* **2009**, *48*, 2877–2880.
(44) Skrabania, K.; Berlepsch, H. v.; Böttcher, C.; Laschewsky, A. *Macromolecules* **2010**, *43*, 271–281.
(45) Dupont, J.; Liu, G. *Soft Matter* **2010**, *6*, 3654–3661.
(46) Ma, Z.; Yu, H.; Jiang, W. *J. Phys. Chem. B* **2009**, *113*, 3333–3338.
(47) Uchman, M.; Stepánek, M.; Procházka, K.; Mountrichas, G.; Pispas, S.; Voets, I. K.; Walther, A. *Macromolecules* **2009**, *42*, 5605–5613.
(48) Kotzev, A.; Laschewsky, A. *Polym. Prepr. (Am. Chem. Soc., Div. Polym. Chem.)* **1998**, *39* (2), 942–943.
(49) Weberskirch, R.; Preuschen, J.; Spiess, H. W.; Nuyken, O. *Macromol. Chem. Phys.* **2000**, *201*, 995–1007.
(50) Kubowicz, S.; Thünemann, A. F.; Weberskirch, R.; Möhwald, H. *Langmuir* **2005**, *21*, 7214–7219.
(51) Zhang, H.; Ni, P.; He, J.; Liu, C. *Langmuir* **2008**, *24*, 4647–4654.
(52) de Gennes, P. G. *C. R. Acad. Sci. Paris, Ser. IIb* **1999**, *327*, 535–538.
(53) Ringsdorf, H. 3rd EURESCO Conference on Supramolecular Chemistry: Molecular Recognition and Drug-Receptor Interactions, Salamanca, Spain, Aug 29−Sept 3, 1996.
(54) Sanchez-Dominguez, M.; Benoit, N.; Krafft, M. P. *Tetrahedron* **2008**, *64*, 522–528.
(55) Kyeremateng, S. O.; Amado, E.; Blume, A.; Kressler, J. *Macromol. Rapid Commun.* **2008**, *29*, 1140–1146.
(56) Taribagil, R. R.; Hillmyer, M. A.; Lodge, T. P. *Macromolecules* **2010**, *43*, 5396–5404.
(57) Schacher, F.; Walther, A.; Müller, A. H. E. *Langmuir* **2009**, *25*, 10962–10969.
(58) Liu, C.; Hillmyer, M. A.; Lodge, T. P. *Langmuir* **2008**, *24*, 12001–12009.
(59) Thünemann, A. F.; Kubowicz, S.; Berlepsch, H. v.; Möhwald, H. *Langmuir* **2006**, *22*, 2506–2510.
(60) Kyeremateng, S. O.; Busse, K.; Kohlbrecher, J.; Kressler, J. *Macromolecules* **2011**, *44*, 583–593.
(61) Kyeremateng, S. O.; Henze, T.; Busse, K.; Kressler, J. *Macromolecules* **2010**, *43*, 2502–2511.
(62) Chou, S.-H.; Tsao, H.-K.; Sheng, Y.-J. *J. Chem. Phys.* **2006**, *125*, 194903.
(63) Xia, J.; Zhong, C. *Macromol. Rapid Commun.* **2006**, *27*, 1654–1659.
(64) Ma, J. W.; Li, X.; Tang, P.; Yang, Y. *J. Phys. Chem. B* **2007**, *111*, 1552–1558.
(65) Zhulina, E. B.; Borisov, O. V. *Macromolecules* **2008**, *41*, 5934–5944.
(66) Ma, Z.; Jiang, W. *J. Polym. Sci., Part B: Polym. Phys.* **2009**, *47*, 484–492.
(67) Kong, W.; Li, B.; Jin, Q.; Ding, D.; Shi, A.-C. *J. Am. Chem. Soc.* **2009**, *131*, 8503–8512.
(68) Xin, J.; Liu, D.; Zhong, C. *J. Phys. Chem. B* **2009**, *113*, 9364–9372.
(69) Zhu, Y.; Kwok, R.; Li, Y.; Jiang, W. *Chem. Phys.* **2005**, *327*, 137–143.
(70) Szczubialka, K.; Moczek, Ł.; Goliszek, A.; Nowakowska, M.; Kotzev, A.; Laschewsky, A. *J. Fluorine Chem.* **2005**, *126*, 1409–1418.
(71) Lodge, T. P.; Rasdal, A.; Li, Z.; Hillmyer, M. A. *J. Am. Chem. Soc.* **2005**, *127*, 17608–17609.
(72) Hansen, C. *Hansen Solubility Parameter: A User's Handbook*, 2nd ed.; CRC Press: Boca Raton, FL, 2007.
(73) Elworthy, P. H.; Florence, A. T.; Macfarlane, C. B. *Solubilization by Surface-Active Agents and Its Applications in Chemistry and Biological Sciences*; Chapman and Hall: London, 1968.
(74) Päch, M.; Zehm, D.; Lange, M.; Dambowsky, I.; Weiss, J.; Laschewsky, A. *J. Am. Chem. Soc.* **2010**, *132*, 8757–8765.
(75) Rizzardo, E.; Chiefari, J.; Chong, B. Y. K.; Ercole, F.; Krstina, J.; Jeffery, J.; Le, T. P. T.; Mayadunne, R. T. A.; Mejis, G. F.; Moad, C. L.; Moad, G.; Thang, S. H. *Macromol. Symp.* **1999**, *143*, 291–307.
(76) Barner-Kowollik, C., Ed.; *Handbook of RAFT Polymerization*; Wiley-VCH: Weinheim, 2008.
(77) Arotçaréna, M.; Heise, B.; Ishaya, S.; Laschewsky, A. *J. Am. Chem. Soc.* **2002**, *124*, 3787–3793.
(78) Donovan, M. S.; Lowe, A. B.; Sumerlin, B. S.; McCormick, C. L. *Macromolecules* **2002**, *35*, 4123–4132.

(79) Baussard, J.-F.; Habib-Jiwan, J.-L.; Laschewsky, A.; Mertoglu, M.; Storsberg, J. *Polymer* **2004**, *45*, 3615–3626.
(80) Bivigou-Koumba, A. M.; Görnitz, E.; Laschewsky, A.; Müller-Buschbaum, P.; Papadakis, C. M. *Colloid Polym. Sci.* **2010**, *288*, 499–517.
(81) Bivigou-Koumba, A. M.; Kristen, J.; Laschewsky, A.; Müller-Buschbaum, P.; Papadakis, C. M. *Macromol. Chem. Phys.* **2009**, *210*, 565–578.
(82) Kempe, K.; Hoogenboom, R.; Hoeppener, S.; Fustin, C.-A.; Gohy, J.-F.; Schubert, U. S. *Chem. Commun.* **2010**, *46*, 6455–6457.
(83) Won, Y.-Y.; Brannan, A. K.; Davis, H. T.; Bates, F. S. *J. Phys. Chem. B* **2002**, *106*, 3354–3364.
(84) Zhang, L.; Eisenberg, A. *Polym. Adv. Technol.* **1998**, *9*, 677–699.
(85) Cameron, N. S.; Corbierre, M. K.; Eisenberg, A. *Can. J. Chem.* **1999**, *77*, 1311–1326.
(86) Webber, S. E. *J. Phys. Chem. B* **1998**, *102*, 2618–2626.
(87) Meli, L.; Lodge, T. P. *Macromolecules* **2009**, *42*, 580–583.
(88) Nyrkova, I. A.; Semenov, A. N. *Macromol. Theory Simul.* **2005**, *14*, 569–585.
(89) Nicolai, T.; Colombani, O.; Chassenieux, C. *Soft Matter* **2010**, *6*, 3111–3118.
(90) Hayward, R. C.; Pochan, D. J. *Macromolecules* **2010**, *43*, 3577–3584.
(91) Choi, S.-H.; Lodge, T. P.; Bates, F. S. *Phys. Rev. Lett.* **2010**, *104*, 047802.